Available online at www.sciencedirect.com

SciVerse ScienceDirect

Ceramics International 38 (2012) 4137–4141

CERAMICS INTERNATIONAL

www.elsevier.com/locate/ceramint

Photoluminescence properties of Tb^{3+} doped Al_2O_3 microfibers via a hydrothermal route followed by heat treatment

Zhenfeng Zhu *, Dianguang Liu, Hui Liu, Xiaofeng Wang, Lu Fu, Dan Wang

School of Materials Science and Engineering, Shaanxi University of Science and Technology, Xi'an 710021, PR China

Received 16 November 2011; received in revised form 5 December 2011; accepted 26 January 2012
Available online 4 February 2012

Abstract

Uniform Al_2O_3:Tb^{3+} microfibers were synthesized via a hydrothermal route and thermal decomposition of a precursor of Tb^{3+} doped ammonium aluminum hydroxide carbonate, and characterized by X-ray diffraction (XRD), scanning electron microscope (SEM), photoluminescence (PL) spectra and decay curves. XRD results indicate that various crystallographic phase Al_2O_3:Tb^{3+} microfibers are obtained by postannealing at different temperatures. SEM results show that the length and diameter of these Tb^{3+} doped α-Al_2O_3 microfibers are about 6–8 μm and 300 nm, respectively. The PL spectra indicate that the $^5D_4 \rightarrow {}^7F_5$ (545 nm) electric dipole transition is the most intensive when excited at 240 nm. It is shown that the 2.0 mol% of doping concentration of Tb^{3+} ions in α-Al_2O_3:Tb^{3+} is optimum. According to Dexter's theory, the critical distance between Tb^{3+} ions for energy transfer was determined to be 12.7 Å. It is found that the decay curves follow the single-exponential decay.

Keywords: B. Fibers; C. Optical properties; D. Al_2O_3

1. Introduction

Conventional fluorescent lamps are gradually being replaced by white LEDs because fluorescent lamps use mercury as an ultraviolet ray source which causes environmental pollution. Compared with conventional fluorescent lamps, the white LEDs have superior properties such as higher luminescence efficiency and environmental friendliness [1–4]. However, the quality of white LEDs is mostly dependent on the red/green/blue (RGB) tricolor phosphors [5,6]. This importance of the phosphors in the development of white LEDs has driven the investigation in the long lasting luminescence of rare earth (RE) doped alumina (Al_2O_3). Al_2O_3 is a suitable host for RE material because it offers a large transparency window from the short ultraviolet to the near infrared frequencies and has excellent mechanical properties and good chemical stability. RE ions doped-Al_2O_3 has been prepared by sol–gel, ion beam implantation, sonochemical, microwave solvothermal, combustion methods [7–14].

Herein, we report the synthesis of Al_2O_3:Tb^{3+} microsfibers via a hydrothermal and postcalcination approach. The luminescence properties under UV are studied in detail and PL spectra indicate that the Al_2O_3:Tb^{3+} microfibers present excellent green emission at 545 nm excited at 240 nm. The optimum concentration and critical distance of Tb^{3+} ions in the Al_2O_3 have been systematically discussed.

2. Experimental

2.1. Synthesis of Al_2O_3:Tb^{3+} microfibers

All the reagents are of the analytical grade without further purification. In a typical synthesis, 8 g poly-glycol (PEG) (Kermel, 99%) with molecular weight Mn = 20,000, was dissolved in deionized water to form a clear solution, to which 7.5 g $Al(NO_3)_3{\cdot}9H_2O$, different amounts of $Tb(NO_3)_3{\cdot}6H_2O$ (0.5, 1.0, 1.5, 2.0, 2.5 mol%) was added. After the salts were totally dissolved, 20 g of urea was added. The mixed solution was further magnetically stirred for 3 h. Then the final mixture was transferred to three Teflon-lined autoclaves of 40-mL capacity and place in an oven at 393 K. After 24 h, the autoclave being cooled to room temperature, the precipitation

* Corresponding author. Tel.: +86 29 86168331; fax: +86 29 86168331.
E-mail addresses: zhuzf@sust.edu.cn, nmlab@sust.edu.cn (Z. Zhu).

0272-8842/$36.00
doi:10.1016/j.ceramint.2012.01.073

were collected and washed several times with deionized water and ethanol to remove the impurities and then dried at 353 K in a vacuum oven for 24 h. In order to study the phase transformation, calcination was also conducted at 773, 1173, and 1473 K in a temperature-programmed Muffle furnace, respectively.

2.2. Characterization

The XRD patterns of the samples were recorded on a high resolution X-ray diffractometer (XRD, D/MAX 2200pc, Japan). Their diffraction patterns were obtained by using Cu Kα radiation of wavelength λ = 0.15418 nm. The morphology of the powder was recorded by using a field-emission scanning electron microscope (JSM-6700F, JEOL Japan) operated at 5 kV. PL, photoluminescence excitation (PLE) spectra and decay curves were carried out with a Hitachi F-4600 fluorescence spectrophotometer at room temperature. In all experiments, both excitation and emission slits were 2.5 nm.

3. Results and discussion

3.1. Crystallization behavior and morphology

The loose powders obtained from aqueous solution, were heat treated at various temperatures for 2 h in a static air atmosphere. The structural analysis by XRD for the as-prepared $NH_4Al(OH)_2CO_3$:Tb^{3+} (2.0 mol%) and Al_2O_3:Tb^{3+} (2.0 mol%) products is used to identify the sample phases and is shown in Fig. 1, curves a–d. As can be seen from Fig. 1, curve a, the clearly distinguishable sharp peaks of the product, prepared by the soft chemical method, are indicative of high crystallinity. All of the diffraction peaks can be neatly indexed to end-centered orthorhombic Ammonium Aluminum Hydroxide Carbonate [$NH_4Al(OH)_2CO_3$] phase (JCPDS No. 76-1923). Under the assistance of PEG-20000 surfactant, the well-crystallized $NH_4Al(OH)_2CO_3$ phase was formed during the hydrothermal treatment process. After thermal decomposition of $NH_4Al(OH)_2CO_3$ at 773 K, amorphous Al_2O_3 is observed (Fig. 1, curve b). Subsequent treatment at 1173 K Fig. 1, curve c shows a pure cubic γ-Al_2O_3 (JCPDS No. 02-1420) with very broad diffraction peaks, indicating a small crystal size. Further increasing the calcination temperature to 1473 K, Fig. 1, curve d shows the most of α-Al_2O_3 (JPCDS No. 78-2427) phase, and the θ-Al_2O_3 (JPCDS No. 23-1009) phase still existed. The crystal size first decreases and then increases with increasing calcination temperature. Using the Scherer equation, the calculated crystal size of $NH_4Al(OH)_2CO_3$, γ-Al_2O_3, α-Al_2O_3 microfibers is about 22.5, 10.8, 32.5 nm, respectively. No other phase is found, because the foreign element, such as carbon and hydrogen from the surfactant, can be oxidized easily at high temperature. Additionally, the concentration of Tb^{3+} is low, and furthermore, Tb^{3+} ions can incorporate into Al_2O_3 lattice and form substituted solid solution. From the analysis results of XRD, the phase evolution of the doping samples can be schematically described as follows with increasing calcination temperature: $NH_4Al(OH)_2CO_3$ → amorphous Al_2O_3 → γ-Al_2O_3 → θ-Al_2O_3 → α-Al_2O_3.

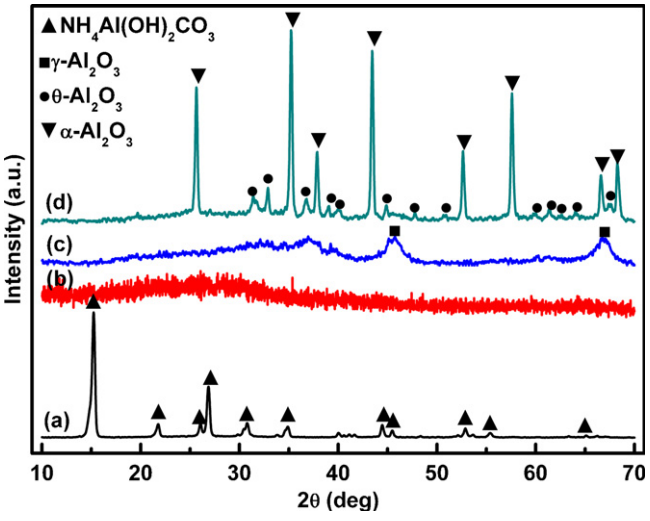

Fig. 1. XRD patterns of the Tb^{3+} doped samples: (a) as-grown from solution and (b–d) postannealed at 773, 1173, 1473 K, respectively.

Differing the dopant levels produced no observable change in the microfibers' size range. Fig. 2 shows selected SEM micrographs of the $NH_4Al(OH)_2CO_3$:Tb^{3+} (2.0 mol%) precursor and the Al_2O_3:Tb^{3+}(2.0 mol%) powders calcined at different temperatures for 2 h. As can be seen from the SEM images, all of the samples consist of uniformly sized microfibers with the length and diameter about 6–8 μm and 300 nm, respectively. The microfibers remain free-standing, remarkably with no sign of aggregation through the whole crystallization process; however, a slight average decrease in diameter is already noticeable. The shrinkage of the diameter is attributed to the pyrolysis of the precursor and the increase of the crystallinity. Moreover, from the SEM investigation, we can see that both the morphology and size of the Al_2O_3:Tb^{3+} microfibers are almost the same as that of the $NH_4Al(OH)_2CO_3$:Tb^{3+} microfibers, implying that the heat treatment has little influence on the morphology of the final products. Thermal treatment only induces $NH_4Al(OH)_2CO_3$:Tb^{3+} into Al_2O_3:Tb^{3+}.

3.2. Luminescence properties of Al_2O_3:Tb^{3+}

Due to the similarities in PLE and PL spectra of the samples with different Tb^{3+} concentrations, typical spectra of Al_2O_3 with 2.0 mol% Tb^{3+} content are shown in the Fig. 3. The PLE spectrum exhibits a broad band with a maximum at about 240 nm, which is due to the $4f^8$–$4f^75d^1$ transitions of Tb^{3+}, and the PL spectrum is characteristic of $^5D_4$–^7F_J transitions for the Tb^{3+} ion [15]. With excitation at 240 nm, three main PL bands, associated with the f–f internal orbital transitions of Tb^{3+} ions, are clearly resolved. They can be related to the radiative transitions from the $^5D_4$ state to ^7F_J (J = 5,4,3) states of Tb^{3+} at 545, 589 and 625 nm, respectively. Nevertheless, for all fabricated samples, the $^5D_4$ → $^7F_5$ (545 nm) electric dipole transition is the most intensive.

Fig. 4 shows the PL spectra of Al_2O_3: Tb^{3+} synthesized at 1473 K for 2 h with different doping concentrations of Tb^{3+}

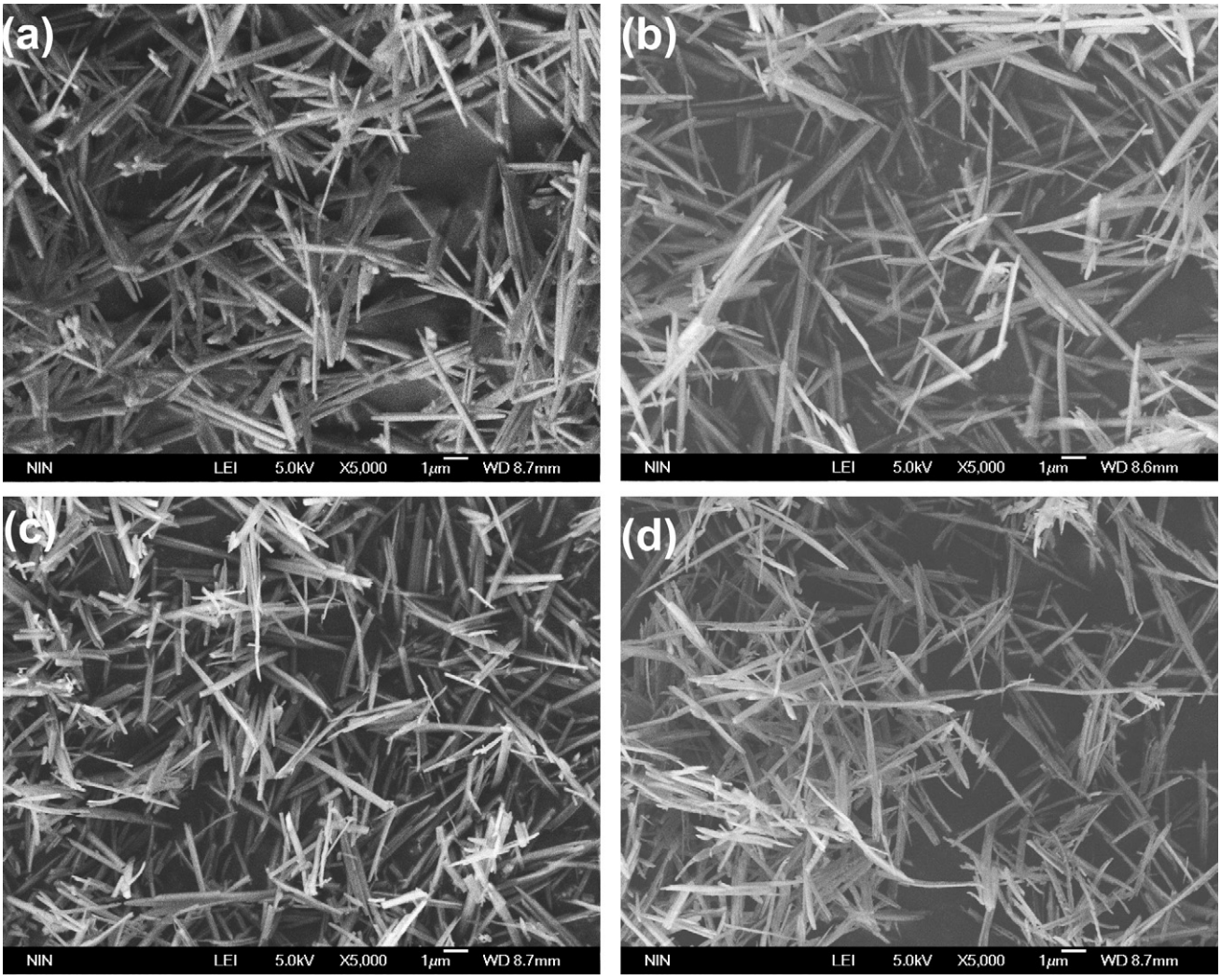

Fig. 2. SEM images of the products: (a) obtained from aqueous solution; (b) postheated at 773 K for 2 h; (c) postheated at 1173 K for 2 h; (d) postheated at 1473 K for 2 h.

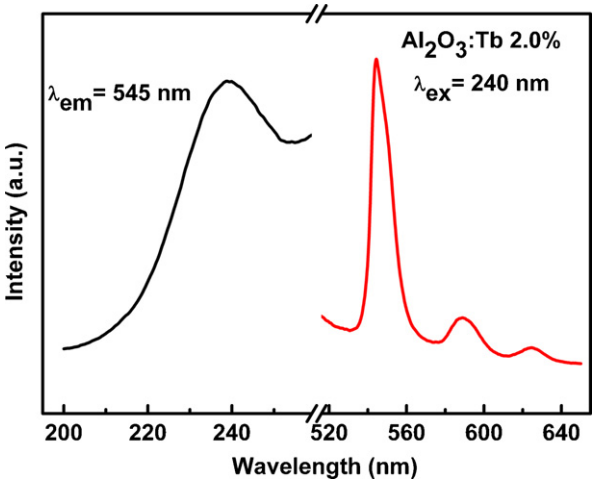

Fig. 3. Room temperature excitation (left) and emission (right) spectra for the Al_2O_3:Tb^{3+} (2.0 mol%) microfibers calcined at 1473 K, measured with a xenon lamp as a light source.

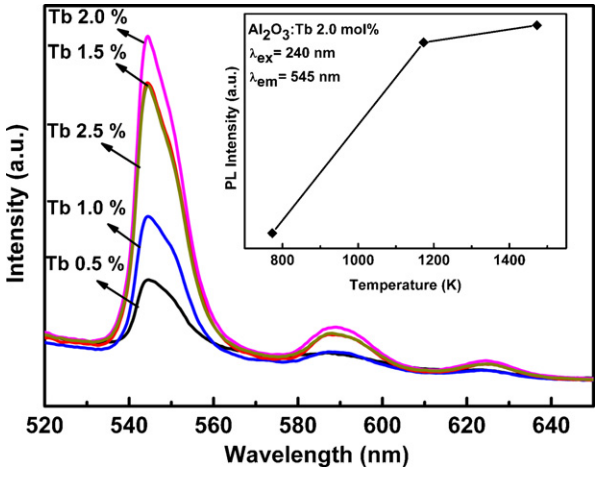

Fig. 4. Emission spectra of Al_2O_3:Tb^{3+} synthesized at 1473 K for 2 h with different doping concentrations of Tb^{3+} (0.5, 1.0, 1.5, 2.0, 2.5 mol%). The inset showing the effect of the postannealed temperatures on the relative PL intensity at 545 nm.

(0.5, 1.0, 1.5, 2.0, 2.5 mol%). Upon excitation at 240 nm, the green emission bands at the wavelength longer than 520 nm are from $^5D_4 \rightarrow {}^7F_J$ ($J = 6, 5, 4, 3$) transitions. The almost alike bands of PL spectra indicate that the symmetry of emitting centers of Tb^{3+} is the same. It is evident that the emission intensity strongly depends on the doping concentration. From the luminescence study the optimum concentration of luminescence is found to be 2.0 mol%. Below this value, the emission intensity is weak because there are no sufficient luminescence centers. The PL reduction for higher doping, the so-called ''quenching'', is a characteristic behavior and inherent to all phosphors [16]. It is based on energy transfer between adjacent luminescent centers [17]. Because the energy levels of similar lanthanide ions match perfectly, this energy transfer is highly efficient and will be favored instead of the light emitting decay [18]. At high doping concentrations, this probability is enhanced [19]. Therefore, based on Dexter's theory [20], the critical distance between Tb^{3+} ions for energy transfer can be calculated by the following relation:

$$R_c \approx 2\left[\frac{3V}{4\pi x_c Z}\right]^{1/3} \quad (1)$$

where V is the volume of the unit cell, x_c the critical concentration of the doping ions and Z the number of host cation in the unit cell. For α-Al_2O_3, $V = 254.7$ Å^3, $Z = 12$ and the critical concentration of Tb^{3+} in the Al_2O_3 host is 0.02. Therefore, the R_c of Tb^{3+} ions is determined to be 12.7 Å.

The inset of Fig. 4 illustrates the evolution of the PL intensity for the $^5D_4 \rightarrow {}^7F_4$ bands as a function of annealing temperature. Doping concentration of Tb^{3+} in the Al_2O_3 host is 2.0 mol%. All of the spectral shapes have no obvious change, because these transitions occur in the f-electron configuration and the 4f shell is well shielded. It is evident that the emission intensity strongly depends on the annealing temperature and increases noticeably for samples annealed above 1173 K. On the basis of the Fig. 1 and inset of Fig. 4, it is noticed that α-Al_2O_3 phase shows more intensive luminescence.

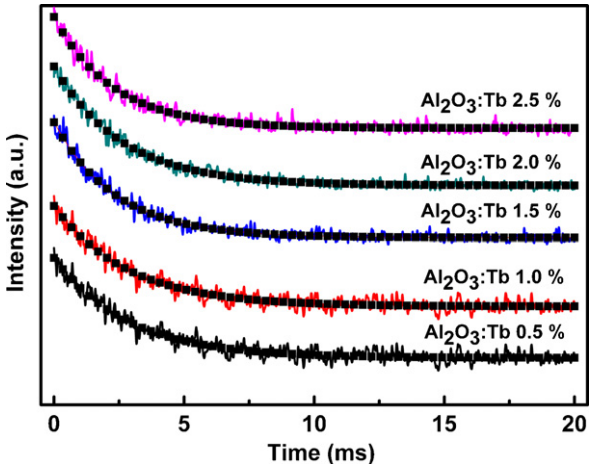

Fig. 5. The decay curves of Al_2O_3:Tb^{3+} phosphors synthesized at 1473 K for 2 h with different concentrations of Tb^{3+} (0.5, 1.0, 1.5, 2.0, 2.5 mol%).

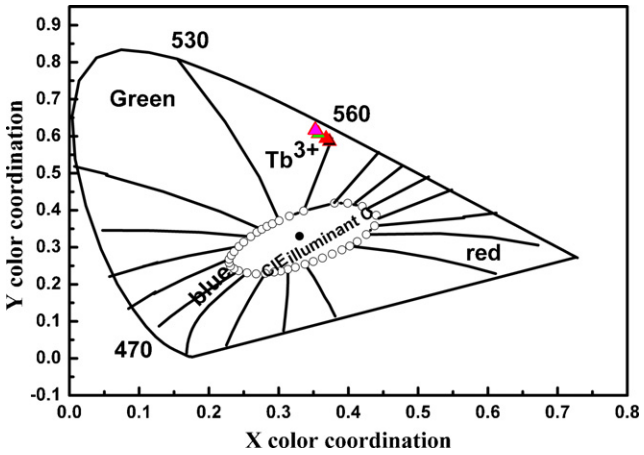

Fig. 6. The CIE coordinates of Al_2O_3:Tb^{3+} phosphors synthesized at 1473 K for 2 h with different concentrations of Tb^{3+} (0.5, 1.0, 1.5, 2.0, 2.5 mol%).

PL decay curves of Al_2O_3: Tb^{3+} with different concentrations of Tb^{3+} (0.5, 1.0, 1.5, 2.0, 2.5 mol%), shown in Fig. 5, were used to calculate the lifetime and investigate the luminescence dynamics of the samples. The samples are excited at 240 nm and monitored at 545 nm, and the curves are obtained with an F-4600 fluorescence spectrophotometer (Hitachi Corp., Tokyo, Japan) under Time Scan mode, and the lifetime values are calculated by the software of the spectrophotometer (FL Solutions for F-4600). It is found that the curves followed the single-exponential decay

$$I_t = I_0 \exp\left(\frac{-t}{\tau}\right) \quad (2)$$

where I_t is the intensity at time t, I_0 is the intensity at $t = 0$, and τ is the decay lifetime. The fitted fluorescence lifetime values of Al_2O_3: Tb^{3+} are 2.460, 2.579, 2.255, 2.783, 2.018 ms corresponding to the Tb^{3+} concentration 0.5, 1.0, 1.5, 2.0, and 2.5 mol%, respectively. The single-exponential decay curves reveal that these bands do not related to the defects of Tb host matrix, which is also confirmed by A. Podhorodecki et al. [21].

The color coordinates for the green emission in the present experiment are calculated based on the corresponding PL spectra and the results are shown in Fig. 6. The coordinates (x, y) of Al_2O_3:Tb^{3+} are (0.368, 0.594), (0.357, 0.607), (0.352, 0.617), (0.353, 0.617), (0.353, 0.616), which correspond to the Tb^{3+} concentration 0.5, 1.0, 1.5, 2.0, and 2.5 mol%, respectively. These results indicate that the as-obtained phosphors could show merits of green emissions in the visible region when excited by a single wavelength light, which is considered to be a promising candidate for application in phosphor-converted LEDs [22].

4. Conclusions

In summary, $NH_4Al(OH)_2CO_3$:Tb^{3+} microfibers were successfully synthesized through a hydrothermal method and Al_2O_3:Tb^{3+} microfibers with different crystalline phases were also obtained by postannealing the resulting precursors at various temperatures. The average length of Al_2O_3:Tb^{3+} microfibers is about 6–8 μm, and the diameter is around

300 nm. These phosphors exhibiting green emission inherit the shapes of the $NH_4Al(OH)_2CO_3$:Tb^{3+} microfibers. The PLE spectrum is dominated by a broad band due to the 4f–4f5d transition of Tb^{3+} ion. For all fabricated samples, the $^5D_4 \rightarrow {}^7F_5$ (545 nm) electric dipole transition is the most intensive. From the luminescence study the optimum concentration of luminescence is found to be 2.0 mol%. The critical energy transfer distance of Tb^{3+} in Al_2O_3 host is calculated to be 12.7 Å. The single-exponential decay curves reveal that these bands do not related to the defects of Tb host matrix. Due to the suitable excitation band, good CIE chromaticity and chemical stability, Al_2O_3:Tb^{3+} phosphor might find potential applications in the fields such as light display systems and optoelectronic devices.

Acknowledgments

This work was financially supported by the China Postdoctoral Science Foundation Founded Project (no. 200902584), the Special Fund from Shaanxi Provincial Department of Education (09JK355), and the Postgraduate Innovation Fund of Shaanxi University of Science and Technology.

References

[1] J.K. Park, K.J. Choi, K.N. Kim, et al., Investigation of strontium silicate yellow phosphors for white light emitting diodes from a combinatorial chemistry, Appl. Phys. Lett. 87 (2005) 031108.

[2] S. Ye, C.H. Wang, X.P. Jing, Photoluminescence and Raman spectra of double-perovskite $Sr_2Ca(Mo/W)O_6$ with A-and B-Site Substitutions of Eu^{3+}, J. Electrochem. Soc. 155 (2008) J148–J150, 151.

[3] H.S. Jang, H. Yang, S.W. Kim, et al., White light-emitting diodes with excellent color rendering based on organically capped CdSe quantum dots and Sr_3SiO_5:Ce^{3+}, Li^+ phosphors, Adv. Mater. 20 (2008) 2696–2702.

[4] R.J. Xie, N. Hirosaki, M. Mitomo, et al., Wavelength-tunable and thermally stable Li-α-Sialon:Eu^{2+} oxynitride phosphors for white light-emitting diodes, Appl. Phys. Lett. 89 (2006) 241103.

[5] W.R. Liu, Y.C. Chiu, C.Y. Tung, et al., A study on the luminescence properties of $CaAlBO_4$:RE^{3+} (RE = Ce, Tb, and Eu) phosphors, J. Electrochem. Soc. 155 (2008) J252–J255.

[6] C.C. Lin, R.S. Liu, Y.S. Tang, et al., Full-color and thermally stable KSrPO4:Ln(Ln = Eu,Tb,Sm) phosphors for white-light-emitting diodes, J. Electrochem. Soc. 155 (2008) J248–J251.

[7] N. Rakov, G.S. Maciel, W.B. Lozano, et al., Investigation of Eu^{3+} luminescence intensification in Al_2O_3 powders codoped with Tb^{3+} and prepared by low-temperature direct combustion synthesis, Appl. Phys. Lett. 88 (2006) 081908.

[8] Z.F. Zhu, D.G. Liu, H. Liu, et al., Fabrication and luminescent properties of Al_2O_3: Tb^{3+} microspheres via a microwave solvothermal route, J. Lumin. 132 (2012) 261–265.

[9] A. Gedanken, R. Reisfeld, L. Sominski, et al., Time-dependence of luminescence of nanoparticles of Eu_2O_3 and Tb_2O_3 deposited on and doped in alumina, Appl. Phys. Lett. 77 (2000) 945–947.

[10] N. Can, P.D. Townsend, D.E. Hole, et al., Enhancement of luminescence by pulse laser annealing of ion-implanted europium in sapphire and silica, J. Appl. Phys. 78 (1995) 6737–6744.

[11] A.A. Kaplyanskii, A.B. Kulinkin, A.B. Kutsenko, et al., Optical spectra of triply-charged rare-earth ions in polycrystalline corundum, Phys. Solid State 40 (1998) 1310–1316.

[12] J.K. Krebs, U. Happek, Yb^{3+} energy levels in α-Al_2O_3, J. Lumin. 94 (2001) 65–68.

[13] A. Pillonnet-Minardi, O. Marty, C. Bovier, et al., Optical and structural analysis of Eu^{3+} doped alumina planar waveguides elaborated by the sol–gel process, Opt. Mater. 16 (2001) 9–13.

[14] T. Ishizaka, R. Nozaki, Y. Kurokawa, Luminescence properties of Tb^{3+} and Eu^{3+}-doped alumina films prepared by sol–gel method under various conditions and sensitized luminescence, J. Phys. Chem. Solids 63 (2002) 613–617.

[15] Y.J. Huang, H.P. You, G. Jia, et al., Hydrothermal synthesis cubic structure, and luminescence properties of $BaYF_5$:RE (RE = Eu, Ce, Tb) nanocrystals, J. Phys. Chem. C 114 (2010) 18051–18058.

[16] G. Blasse, B.C. Grabmaier, Luminescent Materials, Springer, Berlin, 1994.

[17] G. Blasse, The physics of new luminescent materials, Mater. Chem. Phys. 16 (1987) 201–236.

[18] S. Mukherjee, V. Sudarsan, R.K. Vatsa, et al., Effect of structure, particle size and relative concentration of Eu^{3+} and Tb^{3+} ions on the luminescence properties of Eu^{3+} co-doped Y_2O_3:Tb nanoparticles, Nanotechnology 19 (2008) 325704.

[19] R.E. Muenchausen, L.G. Jacobsohn, B.L. Bennett, et al., Effects of Tb doping on the photoluminescence of Y_2O_3:Tb nanophosphors, J. Lumin. 126 (2007) 838–842.

[20] G. Blasse, Energy transfer in oxidic phosphors, Philips Res. Rep. 24 (1969) 131–144.

[21] A. Podhorodecki, M. Banski, J. Misiewicz, et al., Influence of annealing on excitation of Terbium luminescence in $YAlO_3$ films deposited onto porous anodic alumina, J. Electrochem. Soc. 157 (2010) H628–H632.

[22] N.V. Gaponenko, I.S. Molchan, O.V. Sergeev, et al., Enhancement of green Terbium-related photoluminescence from highly doped microporous alumina xerogels in mesoporous anodic alumina, J. Electrochem. Soc. 149 (2002) H49–H52.